

Fabrication of Microelectrodes on Polyester Membranes for Dielectrophoretic Cell Capture

C. Hanke^{a,b}, P. S. Dittrich^b and D. R. Reyes^{a*}

^aSemiconductor and Dimensional Metrology Division, Physical Measurement Laboratory, National Institute of Standards and Technology, 100 Bureau Drive, MS 8120, Gaithersburg, MD 20899, USA

^bDepartment of Chemistry and Applied Biosciences, ETH Zurich, Wolfgang-Pauli-Str. 10, 8093 Zurich, Switzerland

*Corresponding author: darwin.reyes@nist.gov; phone: 301-975-5466; fax: 301-975-5668

ABSTRACT

We present a new system for cell capturing on permeable polyester (PET) membranes using dielectrophoretic forces. Gold microelectrodes were fabricated on PET membranes using conventional photolithographic techniques. Physical characterization by using different microscopy techniques revealed no differences before and after processing. Dielectrophoretic cell trapping was successfully carried out within this microfluidic system and cells remained viable at least a day after capturing.

Keywords: metallization, gold microelectrodes, polyester (polyethylene terephthalate, PET) membrane, dielectrophoresis, cell capture

1 INTRODUCTION

Dielectrophoresis (DEP) has gained a lot of attention, specially in microfluidics, to manipulate particles (e.g., concentration, separation and trapping) due to its (i) label free nature, the (ii) simplicity of the instrumentation, the (iii) favorable scaling effects, and the (iv) ability of applying attracting as well as repulsive forces [1]. Most applications where DEP has been applied to do not require the use of substrates other than the conventional glass or silicon wafers. The microelectrodes on those substrates have been patterned easily using standard photolithographic and metallization techniques. There are few publications on patterning electrodes, for purposes other than DEP, onto soft surfaces. For example, the metallization of nylon membranes was used for sandwich enzyme immunoassays [2]. Additionally, the sputtering process to metallize PET was characterized in more detail [3]. Our work demonstrates the patterning of gold microelectrodes on permeable PET membranes. Ultimately, these patterned microelectrodes were used for dielectrophoretic cell manipulation. We show cell capture by positive DEP and demonstrate that cells were viable 24 h after the DEP trapping experiment was carried out.

2 EXPERIMENTAL SECTION

We used standard photolithographic techniques to metallize the permeable PET membranes. In Figure 1, the fabrication steps are depicted. 1) The PET membrane was fixed on a glass wafer using a 2.25 μm thick layer of poly(methyl methacrylate) (PMMA). 2) Two different photoresists (LOR 3A and S1813) with a thickness of 350 nm and 1.2 μm (respectively) were used to coat the membrane for the bilayer lift-off process. 3) The substrate was exposed to UV-light (150 mJ/cm^2) to transfer the designed microelectrode pattern (1000 μm long, 10 μm wide and 10 μm gaps) onto the photoresists. Next, the pattern was developed in MF-319 for 60 s. During development the LOR 3A undercut the S1813, resulting in stepped edges. The samples were placed in vacuum overnight to ensure that the PET membrane was completely dry. 4) Gold was deposited to a thickness of 50 nm. The stepped edges of the dual photoresist created a discontinuous layer of gold, yielding the desired microelectrode pattern. 5) The photoresists and redundant gold were lifted-off using 1165 remover. The bilayer lift-off was completed within 5 min to 10 min.

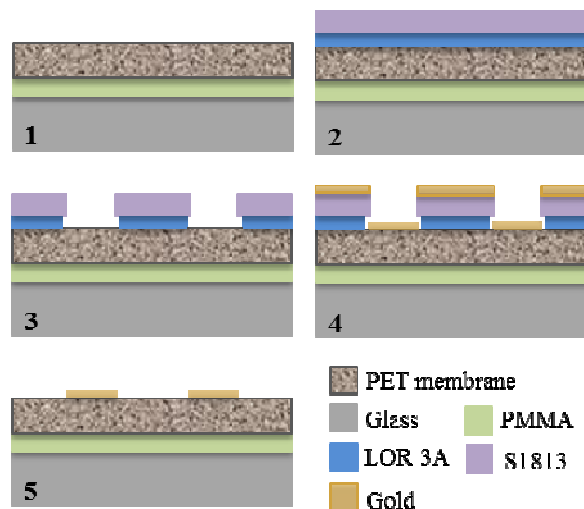


Figure 1. Illustration of the fabrication steps to produce gold microelectrodes on PET membranes.

3 RESULTS AND DISCUSSION

Standard photolithographic processes were used to evaporate and lift-off gold on permeable PET membranes. The dimensions of the resulting interdigitated microelectrode array varied only slightly from the design, yielding a width of $\approx 11 \mu\text{m}$ and gaps between opposite electrodes of $\approx 9 \mu\text{m}$. The processed microelectrodes were characterized by using scanning electron microscopy (SEM), atomic force microscopy (AFM), and optical microscopy to reveal no physical differences before and after processing.

In Figure 2a, a sketch of the patterned design is shown. The microelectrodes (shown in the center) were connected to contact pads, which enabled electrical contact to a waveform generator. Figure 2b-d show SEM images of an actual gold/PET surface. The continuous connection of the patterned gold and the pores (black spots in the coated as well as uncoated areas) can be observed in Figure 2b. In addition, SEM was used to estimate the distance to which gold was deposited inside the pores characterizing their partial blockage. Ten pores were randomly chosen from the area of the surface in Figure 2c (Figure 2d shows one example) and a 2-point z-stack scan was performed to obtain values for the inner (focus on the deepest point of gold inside the pore) and outer (focus on the gold on the surface of the membrane) distance. The average distance to which gold was deposited inside the pores was $2 \pm 1 \mu\text{m}$.

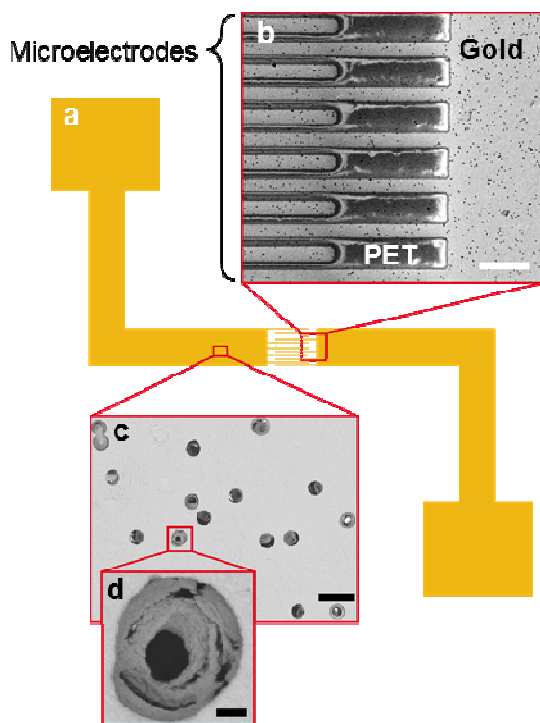


Figure 2. Sketch of the designed pattern of the electrodes and SEM images of the gold patterned membrane. (a) The microelectrodes shown in the center were connected to contact pads. (b) The deposited gold layer (light gray)

formed a continuous layer on the PET membrane (dark gray). The brightest color in the image (on the PET membrane) is due to PET membrane charging during SEM imaging. The pores are observed throughout the entire membrane. (c) The distance to which gold was deposited inside the pores was measured in pores from this surface area. (d) Close up of one pore showing its partial blockage by the deposited gold. (Scale bars: b = $40 \mu\text{m}$, c = $3 \mu\text{m}$, d = 300nm)

AFM imaging (Figure 3) revealed that the metallization of the permeable membrane produced a continuous gold layer on the surface. The pores were visible throughout the entire membrane (average size: $1.2 \mu\text{m}$). Additionally, the RMS (root-mean-square) roughness values were determined on (i) the unprocessed PET membrane, (ii) the processed PET membrane, and (iii) the gold pattern. On each surface seven independent $10 \mu\text{m} \times 10 \mu\text{m}$ squares were imaged and analysed. The RMS roughness on the membrane before and after processing and on the patterned gold were not statistically different ($p > 0.05$).

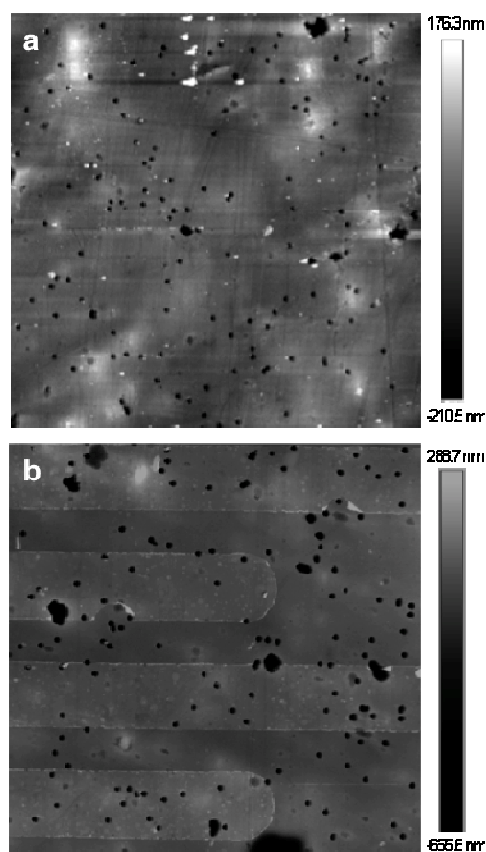


Figure 3. AFM images of PET membranes. In (a) the membrane is shown before and in (b) after depositing gold microelectrodes. Both figures are $75 \mu\text{m} \times 75 \mu\text{m}$. The pores can be nicely observed directly on the PET membrane, but also on the continuous layer of the deposited gold.

Water contact angles were measured during the fabrication process to monitor changes in hydrophilicity. These measurements showed a slight increase in hydrophilicity during processing. However, this should have a positive effect on cell trapping and spreading.

A multilayer microfluidic device was assembled to prove that the permeability of the PET membrane could be restored after processing. Two different food dyes were reversibly exchanged through the pores of the membrane (Figure 4).

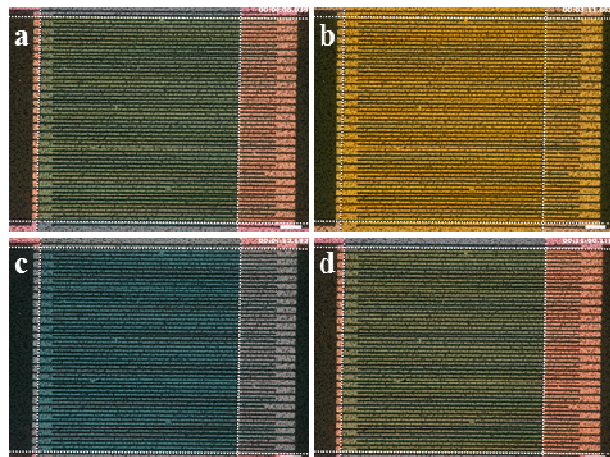


Figure 4. Permeability test of the PET membrane after microelectrode fabrication. A multilayer microfluidic device was used to reversibly exchange yellow and blue food dyes between the channels by their transport through the pores of the intermediate membrane. The white dashed lines indicate the position of the two channels; the yellow dye flowed from left to right and the blue one from top to bottom. (a) At $t = 0$ both flow rates were set to $0.5 \mu\text{l}/\text{min}$,

resulting in a green color at the crossing. (b) The change of the flow rates to $10 \mu\text{l}/\text{min}$ and $0 \mu\text{l}/\text{min}$ (yellow and blue dye, respectively) resulted in the transport of the yellow dye to the blue channel through the membrane and its filling ($t = 3 \text{ min}$). (c) The inverting of the flow rates resulted in the transport of the blue dye to the yellow channel and its filling ($t = 7 \text{ min}$). (d) Both flow rates were set back to $0.5 \mu\text{l}/\text{min}$ and the green color returned at the crossing ($t = 11 \text{ min}$). (Scale bars: $100 \mu\text{m}$)

Ultimately, the electrodes were tested for dielectrophoretic cell capture. Therefore, a microfluidic device was assembled as indicated in Figure 5. The insert shows a micrograph of a fabricated set of microelectrodes. To anchor the cells on the membrane, after switching off the attracting DEP forces, the microelectrodes were coated with polyelectrolyte multilayers (PEMs) as described in [4]. Next, NIH-3T3 cells were harvested in low-conductive media (i.e., $0.147 \text{ mol}/\text{L}$ sucrose) to allow positive DEP. Within 5 min to 10 min the cells were trapped on the microelectrodes and occupied about 50% of this area. Most of these cells (approx. 90%) remained on the microelectrodes on the PEMs/PET surface after switching off the dielectrophoretic forces. The micrographs in the top row of Figure 6 show the cell capture efficiency at various positions. Cell adhesion was significantly higher on the PEMs (only present on the microelectrodes) than in other areas of the channel including the inlet and outlet. A live/dead staining was carried out 24 h after seeding to assess cell viability. Green fluorescence could be observed in approx. 99% of the cells, demonstrating that cells were viable (Figure 6, bottom row).

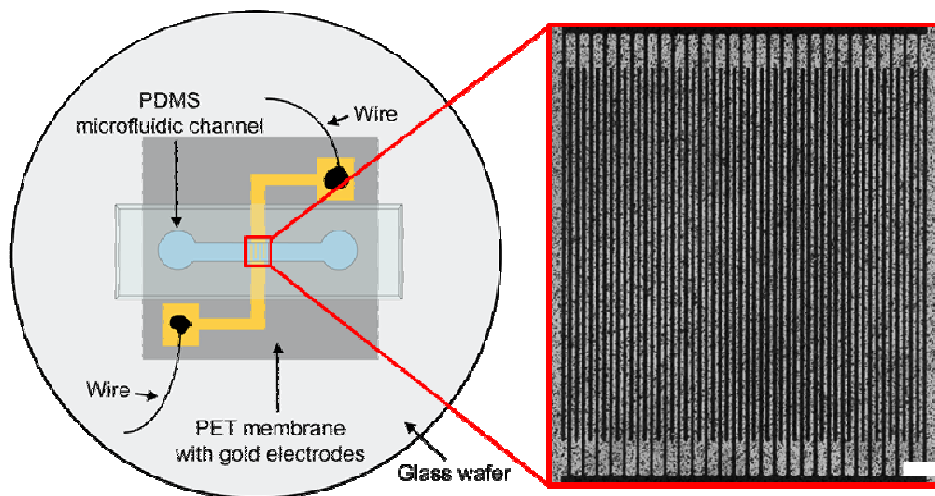


Figure 5. Sketch of the microfluidic device. A piece of PET membrane with deposited gold microelectrodes was fixed onto a glass wafer. The PDMS microfluidic channel is assembled on top, perpendicular to the microelectrodes. The insert shows an actual image of the gold microelectrodes on the PET surface. (Scale bar: $100 \mu\text{m}$)

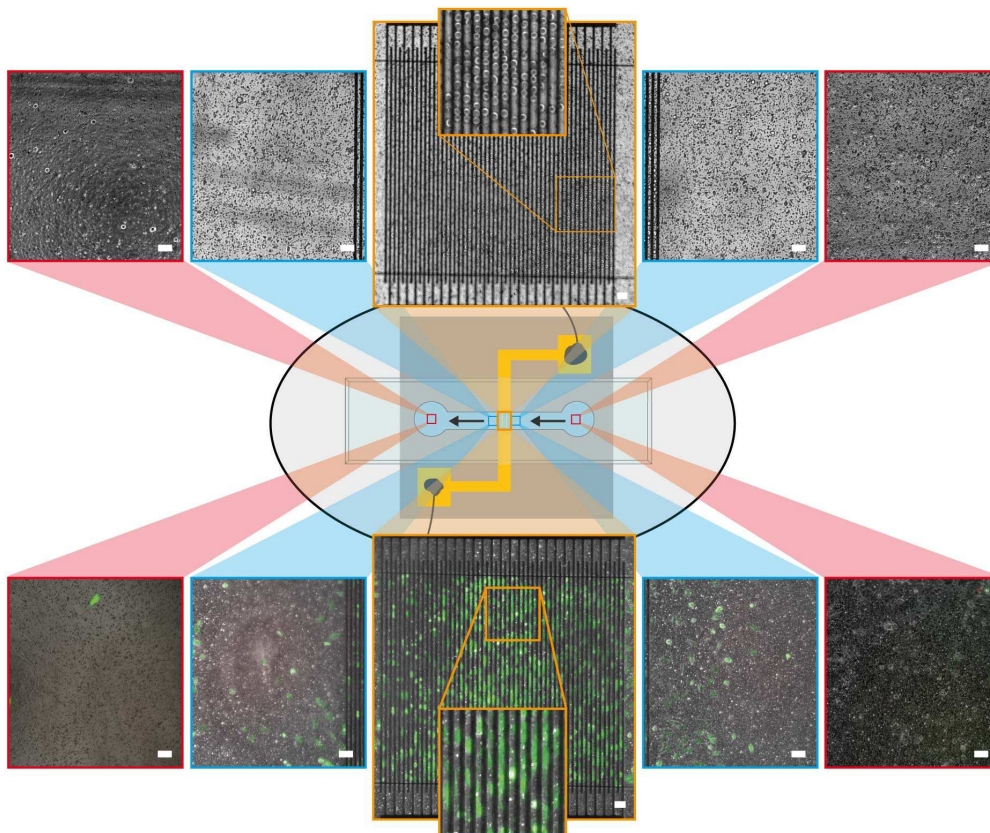


Figure 6. Cell capture using DEP. A sketch of the device is shown in the middle to visualize the locations of the images; the black arrows indicate the direction of the flow. Top row: Micrographs at various positions within the device after switching off DEP forces and exchanging low-conductive media with cell culture media (0 h). NIH-3T3 cell capture was evident within 10 min. Cell adhesion was significantly higher on the PEMs (only present on the microelectrodes). Bottom row: Live/dead staining 24 h after cell capture. The cells spread onto the membrane and green fluorescence could be observed in 99% of the cells, demonstrating that cells were viable. (Scale bars: 50 μm)

4 CONCLUSIONS

The patterning of gold microelectrodes on permeable PET membranes was achieved. The fabrication of these electrodes was carried out using standard photolithographic and metallization processes. We demonstrated the use of these microelectrodes for DEP trapping experiments using NIH-3T3 cells. A cell viability test, performed 24 h after the DEP experiments, demonstrated that 99% of the cells were viable. Our ultimate goal is to combine two different approaches that will facilitate cell studies not envisioned before. We will combine: (i) DEP to capture cells on PEMs for long-term cultivation, and (ii) multilayer microfluidic devices, whereby the two layers are separated by a permeable PET membrane [5]. The fabrication of microelectrodes directly onto the intermediate permeable PET membrane will allow dielectrophoretic cell capture on both sides of the membrane. This microfluidic platform will be a powerful tool to investigate cell-cell interactions and cell co-cultures, where spatial separation and different microenvironments around the cells are a requirement.

5 ACKNOWLEDGEMENTS

C.H. acknowledges the Swiss National Science Foundation for financial support. This work was supported by the NIST Innovations in Measurement Science Cellular Biometry Research Program. This research was performed in part at the NIST Center for Nanoscale Science and Technology. We also thank J-J. Ahn for his support with AFM imaging.

6 REFERENCES

- [1] Cetin B; Li D *Electrophoresis*, 32, 2410-2427, 2011.
- [2] Duan C; Meyerhoff ME *Anal. Chem.*, 66, 1369-1377, 1994.
- [3] Švorčík V; Zehentner J; Rybka V; Slepíčka P; Hnatowicz V *Appl. Phys. A*, 75, 541-544, 2002.
- [4] Reyes DR; Hong JS; Elliott JT; Gaitan M *Langmuir*, 27, 10027-10034, 2011.
- [5] Hanke C; Waide S; Kettler R; Dittrich PS *Anal. Bioanal. Chem.*, 402, 2577-2585, 2012.